Separation of Organic Molecular Mixtures in Carbon Nanotubes and Bundles: Molecular Dynamics Simulations

Zugang Mao and Susan B. Sinnott*,†

Department of Chemical and Materials Engineering, The University of Kentucky, 177 Anderson Hall, Lexington, Kentucky 40506-0046

Received: January 25, 2001; In Final Form: May 17, 2001

Molecular dynamics simulations are used to investigate the diffusive flow of binary molecular mixtures through single-walled carbon nanotubes. Both H-terminated and C-terminated open nanotube ends are considered in the study. The specific mixtures examined are methane/ethane, methane/*n*-butane, and methane/isobutane. The simulations predict which binary mixtures separate as a result of this diffusive flow and which remain mixed and how these results depend on the nanotube properties such as diameter and helical symmetry. The simulations also indicate how the structure and size of the molecules in the mixtures influence the results. For example, *n*-butane and isobutane are predicted to have significantly different separation behaviors when they are mixed with methane molecules. In addition, the degree of separation predicted depends on whether the nanotubes are in bundles.

Introduction

Transport of molecular fluids through porous materials, such as membranes, catalysts, and adsorbents, is of great research interest in the chemical and pharmaceutical industries. These materials generally contain a range of pore sizes, from macro- to micro- to nanopores. Most previous work on these materials has concentrated on fluid transport through macroporous or microporous systems.[1] With the discovery and development of materials such as zeolites[2] and carbon nanotubes,[3] the study of fluid flow through nanopores has increased in recent years.[4−8]

Nanoporous materials already have or are expected to have many industrial applications in adsorption, separation, and catalytic processes involving multicomponent fluids.[9−11] However, determining the mechanism responsible for flow and separation of multicomponent molecular mixtures through nanoporous materials is challenging to accomplish experimentally.[12,13] This is because it is nontrivial to produce nanoporous materials of known pore sizes and distributions. In addition, it is difficult to detect and determine the behavior of molecules inside nanopores. Therefore, computational methods, such as molecular dynamics (MD) or Monte Carlo (MC) simulations, have been widely applied to determine these mechanisms in zeolites and ideal nanopores.[14−17] These theoretical studies play an important role in the analysis of experimental data and provide predictions about molecular mass-transport through the nanopores. Computational studies have shown that molecules confined in nanometer-scale spaces display diffusion properties that are very different from those of bulk fluids. Commonly seen mechanisms include normal-mode diffusion where molecules are able to pass each other,[18] single-file diffusion modes, where molecules are unable to pass each other,[19] and a mode that is between these two that is called transition-mode diffusion.[20]

Our previous MD simulations predicted that transition-mode diffusion in carbon nanotubes and bundles occurs primarily with unsymmetrical molecules such as ethane or ethylene but does not occur for spherical molecules such as methane.[21] Several other research groups[22−33] have studied molecular diffusion or adsorption in carbon nanotubes. Theoretical studies predict that small molecules and noble gas atoms, such as hydrogen, nitrogen, and helium, intercalate into single-walled nanotubes or the interstitial sites between the nanotubes in a bundle.[22−24,27−31] Larger molecules and noble gas atoms, such as xenon, methane, and neon, are predicted to only diffuse inside nanotubes.[32,33] Experimentally, mixtures of methane and krypton have been found to adsorb on the exterior of closed single-walled carbon nanotubes with diameters of 13.3 ± 2 Å at temperatures of about 78 K.[33] It has also been determined that methane molecules can diffuse into single-walled nanotubes with a diffusion coefficient between 3×10^{-7} and 15×10^{-7} cm^2/s at about 90 K.[34]

Numerous other groups[14,35−39] have used computational methods to study the diffusion of molecules in zeolites. The results show that different types of molecules have different adsorption behaviors, with larger molecules usually diffusing by single-file mode and small molecules usually diffusing by normal-mode. Several research groups have also studied the behavior of molecular mixtures in zeolites and other inorganic nanopores. For example, methane/*n*-butane mixtures have been examined in silicalite nanopores by quasielastic neutron scattering experiments and MD simulations and the results indicate that the nono-pore does well at separating the mixture.[40] In addition, MC simulations have recently been used study the adsorption of binary mixtures in carbon nanotubes.[16] The study found that nanotubes preferentially adsorb larger molecules at high temperatures and preferentially adsorb smaller molecules at low temperatures. Finally, the behavior of molecular mixtures in gold nanotubes has been examined.[41] Nanotube diameter, temperature, molecular type, and ratio of mixture components were varied and the resulting separation trends and molecular

* To whom correspondence should be addressed.
† Current address: The University of Florida, Department of Materials Science amd Engineering, P.O. Box 116400, Gainesville, Florida 32611-6400, sinnott@mse.ufl.edu.

10.1021/jp0103272 CCC: $20.00
Published on Web 06/26/2001

adsorption behavior were quantified. The results showed that increasing the diameter of the nanotubes caused the molecular flux to increase and that as the difference in the molecular sizes in the mixture increased, the degree of separation increased as well.

In this paper, we extend our previous classical MD study of molecular diffusion to examine the separation of molecules in individual, single-walled carbon nanotubes and bundles.

Theoretical Approach

The computational approach used is classical MD simulations, where Newton's equations of motion are numerically integrated to track the motion of the atoms with time using a third-order predictor corrector algorithm.[42] The forces on the atoms are calculated using empirical methods that vary with distance. Short-range interactions are calculated using a well-known, many-body, reactive empirical bond-order hydrocarbon potential that realistically describes covalent bonding within both the organic molecules and the carbon nanotubes.[42,43] The long-range interactions are characterized with Lennard−Jones (LJ) potentials.[44] Therefore, the combined expression used to calculate the energy of the system is

$$U = \sum_i \sum_{i<j} [V_r(r_{ij}) - B_{ij} V_a(r_{ij}) + V_{vdw}(r_{ij})] \qquad (1)$$

where U is the binding energy, r_{ij} is the distance between atoms i and j, V_r is a pair-additive term that models the interatomic core−core repulsive interactions, and V_a is a pair-additive term that models the attractive interactions due to the valence electrons. In addition, B_{ij} is a many-body empirical bond-order term that modulates valence electron densities and depends on atomic coordination and bond angles.[45] Finally, V_{vdw} is the contribution from the LJ potential and is only nonzero after the short-range covalent potential goes to zero.

Three binary molecular mixtures are examined in this study. They are methane/*n*-butane, methane/isobutane, and methane/ethane. Four carbon nanotubes are considered: (10,0) with a diameter of 0.80 nm, (8,8) with a diameter of 1.10 nm, (10,10) with a diameter of 1.38 nm, and (12,12) with a diameter of 1.65 nm, where the indexes (n,m) indicate the helical structure of the nanotube.[46] The lengths of all the nanotubes are 10.0 nm and both ends are open and C-terminated unless otherwise indicated. At the start of all the simulations, the molecules are placed near one open end of the nanotube and the system is equilibrated at 300 K. During equilibration, 90% of the atoms in the system have Langevin frictional forces applied to them. Following equilibration, all the atoms in the molecules are allowed to evolve with no constraints while the atoms in the nanotube walls continue to have Langevin frictional forces applied to them. Periodic boundary conditions are applied in the two directions normal to the nanotube axis in order to confine the molecules in a specified volume near the nanotube opening, while leaving motion in the direction of the nanotube axis free. Time steps of 0.25 fs are used and most simulations run for about 150 ps. These conditions are similar to those used to study the diffusion of single molecular species in single-walled carbon nanotubes and bundles.[21,47] Figure 1 shows a snapshot of the start of one of the simulations.

In the analysis of the simulation results, we calculate the flux, density profile, and diffusion coefficient/mobility of the molecules in each system. For each molecular component, the flux of fluid, J, is determined by counting the net number of molecules that cross a given plane of certain area which is normal to the diffusion direction. The equation to calculate J is as follows[48]

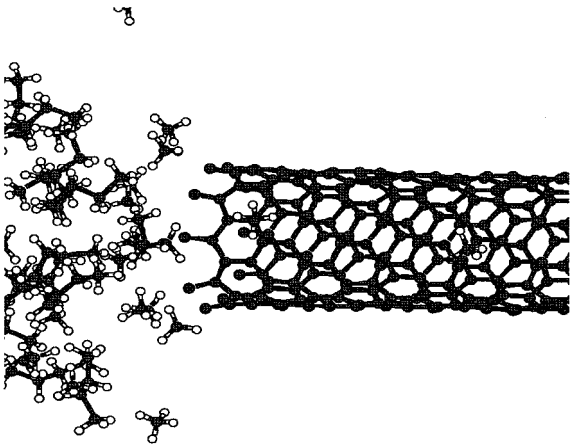

Figure 1. Snapshot at the start of the simulation for a methane/*n*-butane mixture and a (10,0) nanotube.

$$J = \frac{N - N'}{n\Delta t a} \qquad (2)$$

where N is the number of atoms moving from the area of high density to the area of low-density area, N' is the number of atoms moving from the area of low density to the area of high density, n is the number of simulation steps, Δt is the simulation time step, which is 0.25 fs in this study, and a is the area of the cross plane.

The diffusion coefficients or mobilities have different descriptions as the diffusion mode changes. The equation to determine the diffusion coefficient, A, for normal-mode diffusion in single-component systems is as follows[49]

$$A = z^2/2\,t \qquad (3)$$

For single-file diffusion, the mobility, B, is determined from the following[37]

$$B = z^2/\,2\,t^{1/2} \qquad (4)$$

For transition mode diffusion, the mobility, C, is determined as follows[21]

$$C = z^2/\,2\,t^n \qquad (5)$$

In eqs 3−5, z is the average distance that the molecules have moved along the nanotube axis in a given time t.

For multicomponent systems, the diffusion patterns are more complex because of the interactions among different types of molecules. Although the theoretical methods discussed above are still useful, the diffusion behavior will not be identical to the diffusion behavior in single-component systems. Therefore, for multicomponent systems we also use the Onsager theory of irreversible thermodynamic diffusion[50] to describe the relation between the flux and the multidiffusion coefficient. This theory is applicable to multicomponent mixtures in microporous materials when the mechanical interactions between the different components can be neglected. The flux in this case is defined as

$$J_i = -\frac{\rho q^{sat} D_i}{(1 - \Sigma\theta_j)}\left((1 - \sum_{j\neq i}\theta_j)\frac{\partial\theta_i}{\partial z} + \theta_i \sum_{j\neq i}\frac{\partial\theta_i}{\partial z}\right) \qquad (6)$$

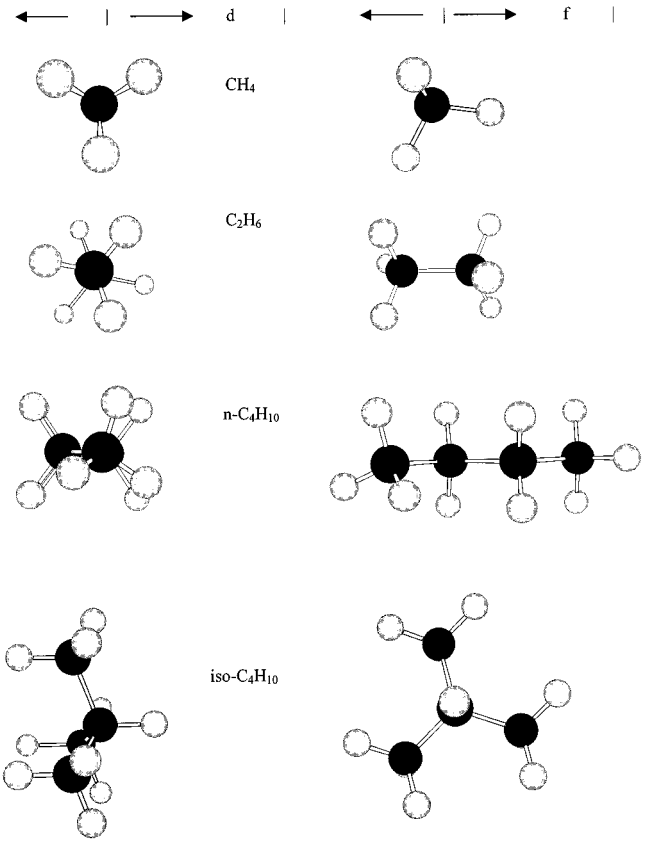

Figure 2. Molecular structures of CH_4, C_2H_6, *n*-C_4H_{10}, and iso-C_4H_{10}. The molecular diameter, *d*, and length, *f*, are also shown for clarity.

The Onsager coefficient is defined as follows

$$L_{ii} = \frac{\rho q^{sat} \theta_i D_i}{RT} \tag{7}$$

where ρ is the molecular density, D_i is the mixed diffusion coefficient for component i, q^{sat} is the saturation volume of the molecules in the nanotubes and θ_i is the fraction of q^{sat} voids occupied by molecule i. This saturation state is calculated under the maximum loading of molecules in the nanotubes. The equation is solved under constant temperature and pressure conditions for the system under consideration. In our analysis of the simulation results we calculate the flux, *J*, using eq 2 directly from the simulations and check the quality of the results using eq 6. The mixed diffusion coefficient D_i here is similar to A of eq 3 but different from B and C of eqs 4 and 5. The Onsager theory is more complicated for cross-coefficients L_{ij} when there is significant mechanical interaction between the different components. These off diagonal Onsager coefficients can be computed from equilibrium MD simulations for arbitrary compositions without mechanical interactions.[51] The separation coefficient, $T_{i/j}$, is used to analyze the separation trends in binary mixtures.[52] We define the separation coefficient as follows

$$T_{i/j} = \frac{\chi_j/\chi_j'}{\chi_u/\chi_i'} \tag{8}$$

here χ_i and χ_j are the mole numbers of components i and j per unit volume at the end of nanotube, respectively, and χ_i' and χ_j' are the initial mole numbers of components i and j, respectively.

In analyzing the results, we also consider the relative sizes of the molecules and Figure 2 shows the structures of CH_4, C_2H_6, *n*-C_4H_{10}, and iso-C_4H_{10}. Two parameters are used in the analysis of molecular size: *d* (the effective diameter of the molecule) and *f* (the effective length of molecules) which are shown in Figure 2. As either *d* or *f* increases, the size of the molecule increases. Furthermore, as the ratio *f*/*d* increases, the linearity of the molecules increases. The values of *d* and *f* for the molecules shown in Figure 2 are listed in Table 1. From the table, the order of molecules with increasing *d* is as follows

$$CH_4 = C_2H_6 < n\text{-}C_4H_{10} < \text{iso-}C_4H_{10}$$

The order of the molecules with increasing *f* is as follows

$$CH_4 < C_2H_6 < \text{iso-}C_4H_{10} < n\text{-}C_4H_{10}$$

Also the order of the molecular linearity with increasing *f*/*d* is as follows

$$CH_4 = \text{iso-}C_4H_{10} < C_2H_6 < n\text{-}C_4H_{10}$$

TABLE 1: Effective Size and Length of the Molecules Considered in the Study

molecular type	*d* (Å)	*f* (Å)	*f*/*d*
CH_4	3.988	3.988	1.00
C_2H_6	3.988	4.755	1.20
n-C_4H_{10}	4.150	8.240	1.99
iso-C_4H_{10}	6.352	6.352	1.00

Results and Discussion

The results of the simulations and analysis are summarized in Table 2 where the results are discussed using the language of single-component systems to better illustrate the mechanisms controlling diffusion. The diameters of the nanotubes and the relative sizes of the molecules are predicted to be the most important criteria for determining molecular adsorption or the diffusion mechanism and the subsequent separation (or lack of separation) of the mixture. The trends that are apparent from the table are as follows: For a given binary mixture, as the diameters of the nanotubes decrease, the amount of separation of the molecular species increases. In addition, as the difference in the relative sizes of the molecules increases, the amount of separation of the molecular species also increases. In all cases, the molecular mixtures are separated by large separation coefficients except for the methane/ethane system.

It should be noted that both diffusion and adsorption are possible in the nanotubes for the larger *n*-butane and isobutane molecules. For the very smallest nanotube diameters considered (0.7−1.1 nm), neither *n*-butane nor isobutane enter the nanotubes because they are too large, whereas the methane diffuses through the nanotubes by normal-mode diffusion. In this case, the diffusion coefficient for methane is almost the same as for the single component cases considered in ref 21. In the medium diameter nanotubes (1.1−1.5 nm), both *n*-butane and isobutane enter the nanotubes but stay in the middle of the pore because there is not enough room for them to get close to the walls due to the relatively high curvature of the nanotube and their relatively large sizes. Therefore, they diffuse down the center of the pore in single-file mode. In the largest diameter nanotubes considered (1.5−2.3 nm), both *n*-butane and isobutane enter the nanotubes and have enough room to get close to the walls and adsorb. Thus, in all three cases separation of the butane/methane mixture occurs. However, the mechanisms are fundamentally different. These simulation results agree with the available experimental data[41] although the systems considered are not identical.

TABLE 2: Summary of Theoretical Results for Diffusion of Molecules and Molecular Mixtures in Carbon-Terminated, Single-Walled Nanotubes[a]

	(10,0)	(8,8)	(10,10)	(12,12)
$CH_4/n\text{-}C_4H_{10}$	CH_4: normal mode $n\text{-}C_4H_{10}$: no motion	CH_4: near normal mode $n\text{-}C_4H_{10}$: single-file mode $T_{CH_4/n-C_4H_{10}}$ is 16.2	CH_4: normal mode $n\text{-}C_4H_{10}$: single-file mode $T_{CH_4/n-C_4H_{10}}$ is 10.6	CH_4: normal mode $n\text{-}C_4H_{10}$: single-file mode $T_{CH_4/n-C_4H_{10}}$ is 8.82
$CH_4/i\text{-}C_4H_{10}$	CH_4: normal mode iso-C_4H_{10}: no motion	CH_4: normal mode iso-C_4H_{10}: single-file mode $T_{CH_4/iso-C_4H_{10}}$ is 25.5	CH_4: normal mode iso-C_4H_{10}: single-file mode $T_{CH_4/iso-C_4H_{10}}$ is 14.3	CH_4: normal mode iso-C_4H_{10}: single-file mode $T_{CH_4/iso-C_4H_{10}}$ is 7.9
CH_4/C_2H_6	CH_4: normal mode C_2H_6: transition mode T_{CH_4/C_2H_6} is 2	both molecules are normal mode T_{CH_4/C_2H_6} is 1.5	both molecules are normal mode T_{CH_4/C_2H_6} is 1.1	

[a] T is the separation coefficient.

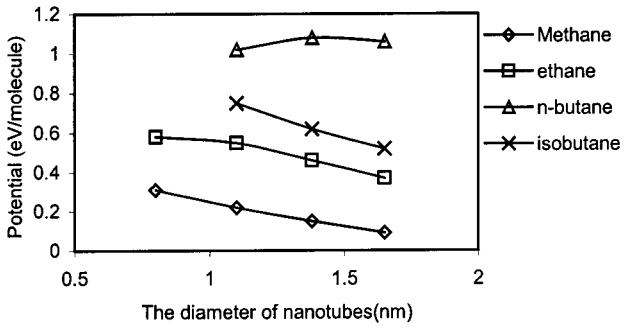

Figure 3. Interaction energy of various molecules in the equilibrium adsorption state on the nanotube walls as a function of the diameter of the nanotubes.

TABLE 3: Effect of Molecular Density on the Results for Methane/*n*-Butane Mixtures in (8,8) and (12,12) Nanotubes

initial molecular density		diffusion coeff or mobility	separation coeff
(12,12)	0.268 g/cm^3	$CH_4 = 3.54 \times 10^{-5}$ cm^2/s $n\text{-}C_4H_{10} = 4.94 \times 10^{-11}$ cm^2/s$^{0.5}$	8.82
	0.147 g/cm^3	$CH_4 = 2.75 \times 10^{-5}$ cm^2/s $n\text{-}C_4H_{10} = 3.28 \times 10^{-11}$ cm^2/s$^{0.5}$	7.63
(8,8)	0.268 g/cm^3	$CH_4 = 14.12 \times 10^{-5}$ cm^2/s $n\text{-}C_4H_{10} = 7.85 \times 10^{-11}$ cm^2/s$^{0.5}$	16.2
	0.147 g/cm^3	$CH_4 = 13.85 \times 10^{-5}$ cm^2/s $n\text{-}C_4H_{10} = 7.81 \times 10^{-11}$ cm^2/s$^{0.5}$	16.1

The equilibrium adsorption energies of individual molecules on interior nanotube walls are considered separately to determine how they compare to one another and how they change with nanotube diameter. Figure 3 shows that the adsorption energy decreases as the nanotube diameter increases for methane, ethane and isobutane. However, in the case of *n*-butane there is a slight increase with nanotube diameter. This is because the *n*-butane's linear structure allows it to line up to an optimum position close to the nanotube wall. The *n*-butane is able to get closer to the nanotube wall when the nanotube has less curvature. Figure 3 also shows that, as expected, the larger molecules have a higher adsorption energy than the smaller molecules.

The effect of changing the initial molecular density on molecular diffusion is examined for the methane/*n*-butane system in (8,8) and (12,12) nanotubes and the results are shown in Table 3. In both cases, the diffusion mode of the molecules does not change with molecular density. However, as the molecular density increases the diffusion coefficient of the methane molecules decreases slightly, whereas the mobilities of the *n*-butane molecules remains almost unchanged in the (8,8) nanotube. Thus, for this nanotube the separation trends remain unchanged. In the lager (12,12) nanotube, the mobility of both butane and methane increases as the molecular density increases leading to smaller separation coefficients.

Figure 4 shows representative plots of the average distance covered by each molecule as a function of time for the methane/ethane mixture in individual (10,0) nanotubes and the methane/*n*-butane, and methane/isobutane systems in individual (10,10) nanotubes. The simulations predict that the mobility of the methane molecules is larger than that of the other molecules. This agrees with published experimental results for methane/*n*-butane mixtures in silicate nanopores.[40] However, at the beginning of the simulation, the methane molecules enter the nanotube more slowly than *n*-butane and so have smaller average displacements at short times. The simulations also predict that the *n*-butane molecules have a larger mobility than isobutene, which agrees with the results of simulations of the diffusion of *n*-butane and isobutane in silicate nanopores.[53] Note that the trends for separation of methane/*n*-butane mixtures and methane/

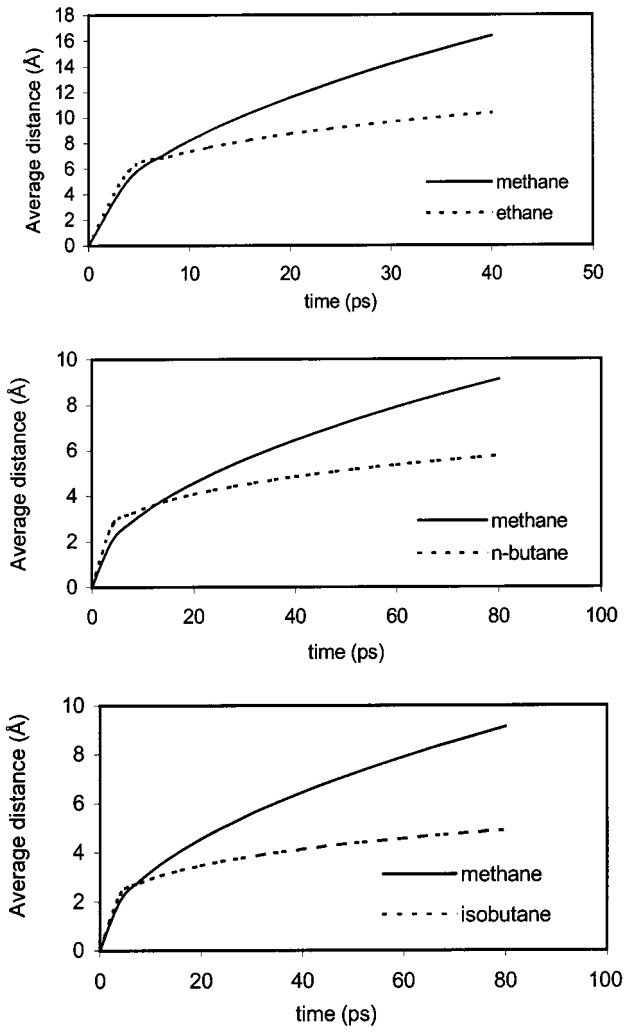

Figure 4. Average distance that the molecules move vs time for the three binary systems considered in this study.

TABLE 4: Comparison of Diffusion Coefficients (the units are cm^2/s) for Methane Molecules in Equilibrium and Averaged over All Molecules (those in equilibrium and those not in equilibrium) over 150 ps at the Densities Indicated

nanotube type	0.268 g/cm^3		0.147 g/cm^3	
	average	equilibrium	average	equilibrium
(10,0)	3.80×10^{-4}	3.55×10^{-4}	3.25×10^{-4}	3.23×10^{-4}
(8,8)	1.86×10^{-4}	1.72×10^{-4}	1.44×10^{-4}	1.41×10^{-4}
(10,10)	9.54×10^{-5}	9.29×10^{-5}	7.70×10^{-4}	7.64×10^{-4}
(12,12)	3.56×10^{-5}	3.12×10^{-5}	2.45×10^{-5}	2.38×10^{-4}

isobutene mixtures are not identical. A comparison of mixed molecular systems and single-component systems shows that the diffusion coefficients of small molecules decrease and the mobilities of large molecules increase in the mixed molecular systems relative to the single-component systems at the same molecular density.

The conditions in these simulations are those of nonequilibrium MD because the molecular density of the first molecules to enter the nanotube differs from the density of the molecules that follow. Equilibrium MD is often used to compute transport diffusivity efficiently and has shown good agreement with experimental data in zeolites.[54,55] We have therefore reanalyzed the simulation results and examined the diffusion of only the molecules in equilibrium with each other and their surroundings and for which the environment, including molecular density, is identical. As the molecular density increases, the time needed to achieve equilibrium varies from 4 to 20 ps. The equilibrium diffusion coefficients for methane at various densities and diffusing in various nanotubes are shown in Table 4 and are compared with the average (equilibrium and nonequilibrium) diffusion coefficients for methane in the same nanotubes. The results show that the equilibrium diffusion coefficients are almost the same as the average values at the lower molecular density of 0.147 g/cm^3. At the higher molecular density of 0.268 g/cm^3, the equilibrium values are about 5 to 8% lower than the average value.

As the diameters of the nanotubes increase from that of the (10,10) nanotube, the amount of separation decreases as almost all of the molecules enter the nanotube, as shown in Table 2. From (10,0) to (12,12), the separation coefficient decreases for the methane/*n*-butane and methane/isobutane systems. The reason for this decrease is that the isobutane and *n*-butane molecules now have room to adsorb to the nanotube walls, although *n*-butane adsorbs more strongly than isobutane because its larger *f*/*d* ratio allows the bonds in the molecule to align with the carbon−carbon bonds in the nanotube. Neither methane nor isobutane can get as close to the nanotube walls because of their smaller *f*/*d* ratios. When *n*-butane and isobutane adsorb to the walls, they partially block the pore and make it more difficult for methane to go through, in agreement with the findings of ref 40.

The diffusion behavior of the methane molecules in the binary mixtures is analyzed relative to the single-component system studied in ref 21. The results show that the diffusion coefficients of methane in the binary systems are significantly smaller than in single-component systems when the size difference between methane and the molecule it is mixed with is large. The reason for this change is that the interactions of the methane molecules with the isobutane or *n*-butane molecules are significantly stronger than the methane−methane interactions and thus slow the diffusion of methane.

Figure 5 shows the density profile of the molecular mixtures in (8,8) and (10,10) nanotubes after 150 ps. From the figure, it is clear that the density profile of methane is linear in the two binary systems inside the (10,10) nanotubes which indicates that methane diffuses by normal-mode diffusion. However, in the (8,8) nanotubes the density profile of methane is not linear when it is mixed with *n*-butane or isobutane indicating that methane diffusion is not strictly normal-mode in these cases. In this case, the Onsager equation is more suitable because molecular interactions between the methane and butane are strong and thus perturb the molecular diffusion of methane in smaller diameter nanotubes. In (10,10) nanotubes, methane and ethane both follow standard normal-mode diffusion. However, in (8,8) nanotubes methane follows normal-mode diffusion while ethane follows single-file diffusion. Thus, in this case the behavior of both molecules is similar to the results of single-component methane and ethane fluids obtained previously.[21] This means that as the size difference between the molecules decreases, the effect of methane's interactions with the other molecule in the mixture also decreases.

These three trends illustrate the fact that in molecular diffusion through carbon nanotubes there are two factors that seem to most affect the diffusion behavior of molecules: one is the interaction between the molecules and the nanotube walls and the other is the interaction among the molecules themselves. The main driving force for diffusion is the first type of interaction listed. However, intermolecular interactions can have profound effects on the diffusion mechanism followed by a certain type of molecule. This is especially apparent in binary molecular mixtures where different types of molecules have different effects on each other during diffusion. This effect will increase as the size difference between different molecules increases. For methane/ethane mixtures, the behavior of both molecules is similar to their behavior in single-component systems. However, there are more significant differences in the behavior of methane in methane/butane systems.

Figure 6 shows the average density profile at the cross section of the nanotubes in three binary systems in (8,8) and (12,12) nanotubes. In the (8,8) nanotubes, the methane and other molecules mix with each other. As the diameters of the nanotubes increase, the molecules separate with the methane concentrated near the center of the pore while the butane molecules concentrate near the walls. This separation trend is clearly seen in the density plot for the (12,12) nanotube. We also examine the effect of molecular linearity on the separation of the methane/ethane mixture. Although the size difference between the methane and ethane molecules is small there is a significant difference in molecular linearity *f*/*d*. Therefore, methane and ethane also tend to separate from each other. More ethane molecules are concentrated near the wall in larger diameter nanotubes than in smaller diameter nanotubes, which increases the degree of separation from methane. By contrast, in the (8,8) nanotubes both methane and ethane are forced into the center of the nanotube by the constrained size and large curvature of the pore. Thus, the effect of linearity increases as the diameter of the nanotubes increases.

Figure 7 shows the flux along the nanotube axis at 150 ps. It is seen that in the (10,10) nanotubes, the flux of methane is almost the same throughout the entire nanotube and the diffusion coefficient of methane is constant in the nanotubes. In contrast, for both *n*-butane and isobutane, the flux decreases sharply along the nanotube axis as the butane molecules attach to the walls of the nanotubes. In the case of the methane/ethane mixture, the separation trend is not significant in our simulations because their size difference is small. However, in the (8,8) nanotubes, only methane follows normal mode diffusion while ethane follows similar transition-mode diffusion pattern.

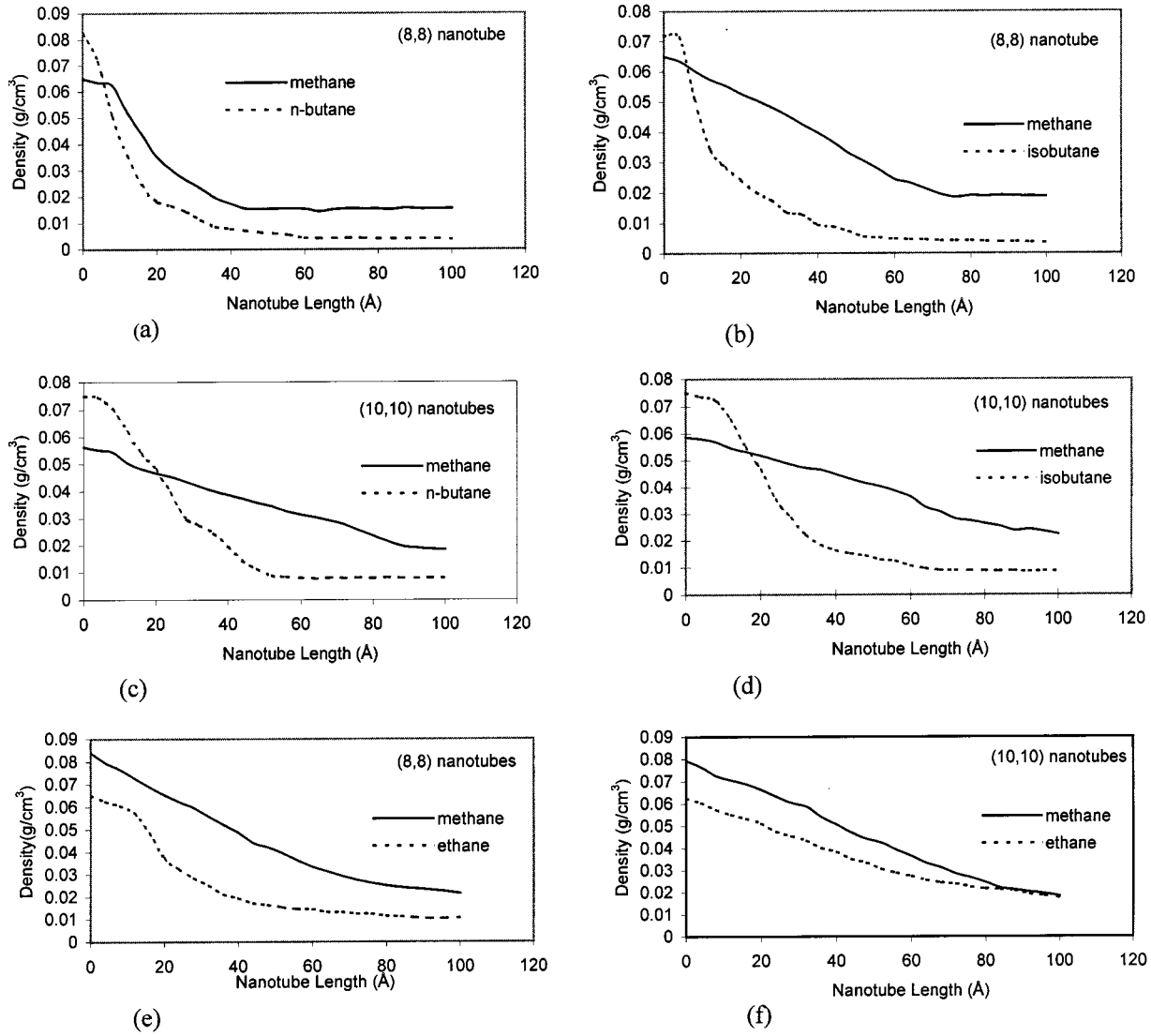

Figure 5. Density profile of the molecules in the (8,8) and (10,10) nanotubes after 150 ps at 300 K.

Next, the Onsager formulation is used to determine the Onsager diffusion coefficient. Figure 8 shows the Onsager diffusion coefficient D_i as a function of molecular density for methane/*n*-butane mixtures in (8,8) and (12,12) nanotubes. In the (8,8) nanotubes, the coefficients of both molecules increase slightly as the molecular density increases. In contrast, in the (12,12) nanotubes, the coefficients of both molecules increase sharply as the molecular density increases. Note that the Onsager equation provides the mixed diffusion coefficient in the same units for both types of molecules making it easier to compare the two. Examination of the D_i values for the two molecules shows that $D_{n-C4H10}$ increases more than D_{CH4} as the molecular density increases. This agrees with the decrease in the separation coefficients as the density increases.

A comparison is made between the binary Onsager diffusion coefficient for the mixture from eq 6 and the diffusion coefficient of methane from eq 2. The results are shown in Table 5. The comparison shows that the two results are similar. In the (12,12) nanotubes, both *D* and *A* increase as the molecular density increases. In the (8,8) nanotubes, *A* increases slightly, and *D* decreases as molecular density increases. The reason for these trends is that the loading of molecules inside the nanotubes changes with the molecular density. As the molecular density changes in small diameter nanotubes, the loading of the butane molecules goes up, which hampers the motion of the methane molecules. This causes the degree of molecular separation to decrease, despite the fact that the loading of the methane is also increasing. The interference in the diffusion of the methane from the increased presence of butane cancels the density-gradient driving force on the molecules in nanotubes with smaller diameters. Therefore, the diffusion coefficient of methane changes little with changes in molecular density in (8,8) nanotubes. As the size of nanotubes increases, the density-gradient driving force becomes stronger and the diffusion coefficients of both methane and butane increase. It should be pointed out here that the difference between *A* and *D* is due to the fact that the Onsager diffusion coefficient corresponds to the equilibrium diffusion state in the nanotubes, whereas *A* is the average value for molecules in nonequilibrium and equilibrium conditions.

The effect of the initial composition ratio of the molecules in the mixtures is illustrated in Figure 9 which shows the separation coefficients vs the mole ratio for each set of molecules. The simulations show that as the ratio of methane to butane increases, the absolute amount of methane increases but the separation coefficients just increase slightly. This ratio does not have a significant effect on the separation trends for the systems. As the ratio increases in the (8,8) nanotubes, the diffusion mode of methane approaches strict normal-mode diffusion. Thus, as the ratio of concentration of the two

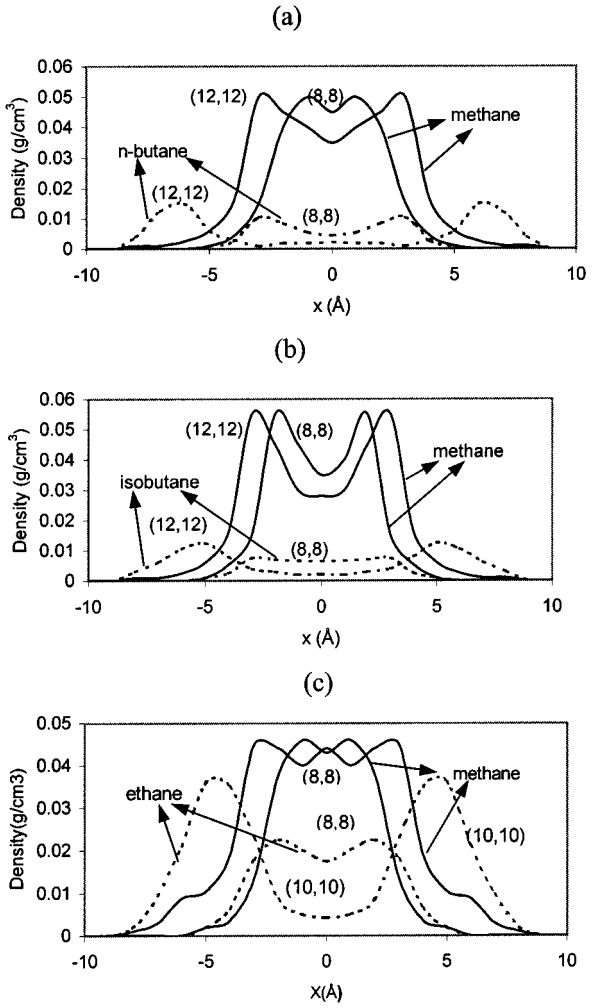

Figure 6. Average density profile of the nanotubes in (8,8) and (12,12) nanotubes after 150 ps at 300 K (a) methane/*n*-butane, (b) methane/isobutene, and (c) methane/ethane.

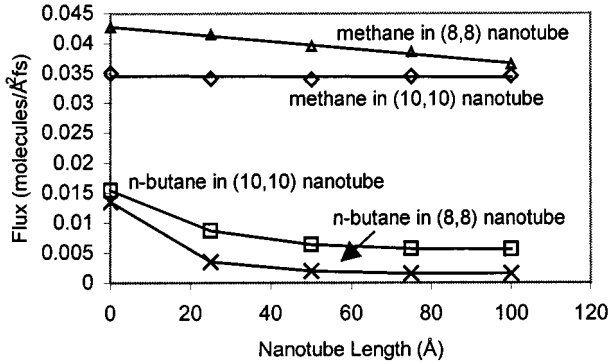

Figure 7. Flux along the nanotube axis in (10,10) nanotubes for methane/*n*-butane and methane/isobutane systems at 300 K.

molecules increases, the concentration of butane molecules decreases, and the behavior of the binary system converges to that of the single-component systems.

The effect of the helical structure of the carbon atoms within the nanotube walls is also considered in this study. Two helical patterns were considered: zigzag with (*n*, 0) indexes and armchair with (*n*,*n*) indexes.[47] To isolate the effect of helical structure, diffusion in two nanotubes of similar diameter were considered: (14,0) a zigzag nanotube with a diameter of 1.11 nm and (8,8) an armchair nanotube with a diameter of 1.10 nm. The results for these two cases are found to be the same.

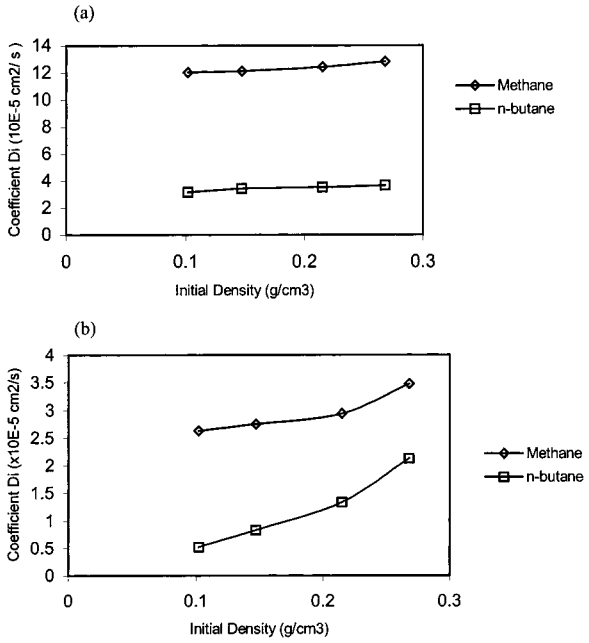

Figure 8. Onsager diffusion coefficient vs initial molecular densities (a) in (8,8) and (b) in (12,12) nanotubes.

TABLE 5: Comparison of Diffusion Coefficients *A* from Eq 3 and *D* from Eq 6 of Methane under Different Initial Molecular Densities

nanotube type	(8,8)		(12,12)	
initial density (g/cm^3)	0.147	0.268	0.147	0.268
D (cm^2/s)	12.15×10^{-5}	12.83×10^{-5}	2.93×10^{-5}	3.48×10^{-5}
A (cm^2/s)	14.12×10^{-5}	13.85×10^{-5}	2.75×10^{-5}	3.54×10^{-5}

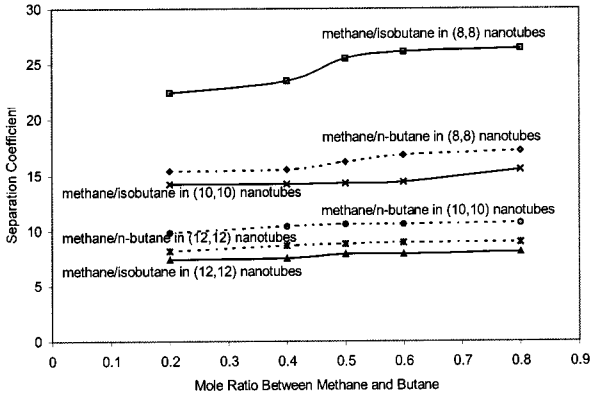

Figure 9. Separation coefficients vs the mole ratio of two types of molecules in molecular mixtures of methane/isobutane and methane/*n*-butane in (8,8), (10,10), and (12,12) nanotubes at 300 K.

TABLE 6: Comparison of Separation Coefficients for Molecular Mixtures in Armchair and Zigzag Nanotubes of Comparable Diameter

nanotube type	(14,0)	(8,8)
methane/*n*-butane	15.8	16.2
methane/isobutene	24.9	25.5

Table 6 shows the separation coefficients of methane/*n*-butane and methane/isobutene systems in both nanotubes, and they are found to be close in value. Thus, the helical structure of carbon nanotubes does not have an effect on the diffusion behavior of binary molecular mixtures for the diameters considered in this study. Similar results were predicted in our study of single component systems.[21]

TABLE 7: Comparison of Separation Coefficients for Methane/*n*-Butane in Nanotubes with Different Atomic-Terminations at the Nanotube Opening

nanotube type	(8,8)	(10,10)
C-terminated	16.2	10.6
H-terminated	15.7	9.1

TABLE 8: Comparison of the Separation Trends of a Methane/*n*-Butane Mixture in an Individual Single-Walled Nanotube and a Single-Walled Nanotube Bundle

individual (10,0) nanotube	bundle of (10,0) nanotubes
CH_4: normal-mode diffusion	CH_4: normal-mode diffusion
n-C_4H_{10}: no motion on these time scales	*n*-C_4H_{10}: single-file mode diffusion
	$T_{methane/n-butane}$ is 18
diffusion coeff of CH_4 = 3.52×10^{-4} cm^2/s	diffusion coeff of CH_4 = 2.52×10^{-4} cm^2/s
	mobility of *n*-C_4H_{10} = 8.95×10^{-10} cm^2/s$^{0.5}$

The effect of the termination edge of the carbon nanotubes on the results is also investigated. Two types of atomic-termination at the nanotube edges are considered: C-termination and H-termination. The effect of edge-termination is summarized in Table 7. For methane/*n*-butane systems, the results show little effect on the separation trends. However, they also show that the molecules enter the C-terminated nanotubes more rapidly than the H-terminated nanotubes. This is because the C-terminated edges are more reactive than H-termination and have attractive long-range interactions with the diffusing molecules.

Finally, diffusion in a bundle of single-walled carbon nanotubes is considered. The bundle consists of three close-packed (10,0) nanotubes where the distance between the nanotubes is 0.34 nm. Similar separation trends are predicted as are seen in single (10,0) nanotubes. The diffusion coefficient of methane is about $^1/_4$ smaller in the bundle than in the single (10,0) nanotube (3.52×10^{-4} cm^2/s for methane in the single nanotube and 2.52×10^{-4} cm^2/s in the nanotube bundle). No molecules are predicted to diffuse into the interstitial sites in the bundle, due to the relative interaction potentials between the molecules and the nanotubes. This interaction is -0.24 eV/molecule inside the nanotubes and -0.16 eV/molecule between the nanotubes for methane.[21] For a single nanotube that is not part of a bundle, the potential is -0.31 eV/molecule for methane.[21] Thus, the nanotube−nanotube interactions have a significant effect on the molecular diffusion by altering the molecule's interaction potential with the nanotube walls. These results agree with the calculations in ref 24 that found that the binding energies inside individual nanotubes are higher than in nanotubes that are within bundles. In other words, nanotube−nanotube interactions result in increased molecular activity inside the nanotube pore.

The separation results of the methane/*n*-butane system in an individual (10,0) nanotube and a bundle of (10,0) nanotubes are shown in Table 8. The diffusion coefficients of methane are about 28% smaller in nanotube bundles compared to individual nanotubes. In this bundle, some *n*-butane molecules diffuse through the nanotubes although the separation coefficient is quite large. This is in contrast to their behavior in individual (10,0) nanotubes, where none of the butane molecules enter the pore. In the (10,0) nanotubes in the bundle, *n*-butane diffuses by single-file mode, whereas the methane molecules follow normal-mode diffusion.

Conclusions

Molecular dynamics simulations are used to investigate the diffusion of binary molecular mixtures through carbon nanotubes and bundles, and the following conclusions can be drawn. Molecular structure has a large effect on the separation and diffusion behavior of binary molecular systems in nanotubes. Both *n*-butane and isobutane separate well from methane through diffusion but the diffusion coefficients for these two butane structures are significantly different from one another. In addition, the helical structure of the nanotube walls is predicted to have no effect on the diffusion behavior of molecular mixtures, but the diameter of the nanotube has a large effect on the results. As the diameter of the nanotubes increases, the amount of separation between the molecules decreases. The amount of separation in the methane/isobutene system is larger than in the methane/*n*-butane system because the former has a larger difference of molecular size.

N-butane adsorbs more readily to the interior nanotube walls than isobutane because of its linear structure. There is therefore more probability that *n*-butane molecules will align along the nanotube walls. Hence, the average distance between the nanotube wall and *n*-butane molecules is shorter than in the case of isobutane, so the interactions between the pore walls and the *n*-butane molecules are stronger than the interactions of the pore walls with isobutene.

For the methane/ethane system, the diffusion behavior of both molecules is similar to their behavior in single-component fluid systems because their size difference is small.

Different terminations of the carbon nanotubes have little effect on the separation trends. The molecules have more difficulty diffusing into H-terminated nanotubes than C-terminated nanotubes. However, the separation trends do not change with atomic termination. In nanotube bundles, the diffusion behavior and coefficients of binary molecular systems changed relative to the diffusion behavior in individual nanotubes.

Thus, carbon nanotubes can be used to separate methane/*n*-butane and methane/isobutane mixtures. However, these separations are largest when the diameters of the nanotubes are smaller. Methane/ethane mixtures do not show significant separations in the nanotubes considered in the study.

Acknowledgment. This work was supported by the Advanced Carbon Materials Center at the University of Kentucky which is funded by the National Science Foundation through Grant No. DMR-9809686, and by the NASA Ames Research Center through Grant No. NAG 2-1121. The authors thank D. Sholl, P. Keblinski, E. Grulke, M. Jagtoyen, and F. Derbyshire for many helpful discussions.

References and Notes

(1) Jackson, R. *Transport in Porous Catalysts*; Elsevier: New York, 1997.
(2) Karger, J.; Ruthven, D. M. *Diffusion in Zeolites and Other Microporous Solids*; John Wiley & Sons: New York, 1992.
(3) Iijima, S. *Nature* **1991**, *354*, 56.
(4) de Vos, R. M.; Verweij, H. *Science* **1998**, *279*, 1710.
(5) Gergidis, L. N.; Theodorou, D. N. *J. Phys. Chem. B* **1999**, *103*, 3380.
(6) Mohanty, S.; McCormick, A. V. *Chem. Eng. J.* **1999**, *74*, 1.
(7) Thomson, K. T.; Wentzcovitch, R. M. *J. Chem. Phys.* **1998**, *108*, 8584.
(8) Mason, E. A.; Malinauskas, A. P. *Gas Transport in Porous Media: The Dusty Gas Model*; Elsevier: Amsterdam, 1983.
(9) Breck, D. W.; Krieger, R. E. *Zeolite Molecular Sieves*; Publishing Co: Florida, 1974.
(10) Sircar, S.; Myers, A. L. *Surf. Sci.* **1988**, *205*, 353.
(11) . Keffer, D.; Davis, H. T.; McCormick, A. V. *J. Phys. Chem.* **1996**, *100*, 638.
(12) Weitkamp, J.; Olhamnn, G.; Vedrine, J. C.; Jacobs, P. A. *Catalysis and Adsorption by Zeolites*; Elsevier: Amsterdam, 1991.
(13) Chen, N. Y.; Degnan, T. F.; Smith, C. M. *Molecular Transport and Reaction in Zeolites*; VCH Publishers: New York, 1994.

(14) Keffer, D.; McCormick, A. V.; Davis, H. T. *Mol. Phys.* **1996**, *87*, 367.
(15) Tuzun, R. E.; Noid, D. W.; Sumpter, B. G.; Merkle, R. C. *Nanotechnology* **1997**, *8*, 112.
(16) Ayappa, K. G. *Langmuir* **1998**, *14*, 880.
(17) Khan, I. A.; Ayappa, K. G. *J. Phys. Chem.* **1998**, *109*, 4576.
(18) Nelson, P. H.; Scott, M. A. *J. Chem. Phys.* **1999**, *100*, 9235.
(19) Sholl, D. S.; Fichthorn, K. A. *J. Chem. Phys.* **1997**, *107*, 4394.
(20) Sholl, D. S. *Chem. Eng. J.* **1999**, *74*, 25.
(21) Mao, Z.; Sinnott, S. B. *J. Phys. Chem. B* **2000**, *104*, 4618.
(22) Stan, G.; Bojan, G. M.; Curtarolo, S.; Gatica, S.; Cole, M. *Phys. Rev. B* **2000**, *62*, 2173.
(23) Stan, G.; Hartman, J.; Crespi, V.; Gatica, S.; Cole, M. *Phys. Rev. B* **2000**, *61*, 7288.
(24) Cole, M.; Crespi, V.; Stan, G.; Ebner, C.; Hartman, J.; Moroni, S.; Bninsegni, M. *Phys. Rev. Lett.* **2000**, *84*, 3883.
(25) Green, D.; Chamon, C. *Phys. Rev. Lett.* **2000**, *85*, 4128.
(26) Lefebvre, J.; Antonov, R.; Radosavljevi, M.; Lynch, J.; Llaguno, M.; Johnson, A. T. *Carbon* **2000**, *38*, 1745.
(27) Simonyan, V.; Diep, P.; Johnson, K. *J. Chem. Phys.* **1999**, *111*, 9778.
(28) Yin, Y.; Mays, T.; McEnaney, B. *Langmuir* **1999**, *15*, 8714.
(29) Gatica, S.; Cole, M.; Stan, G.; Hartman, J.; Crespi, V. *Phys. Rev. B* **2000**, *62*, 9989.
(30) Dillon, A.; Jones, K.; Bekkedahl, T.; Kiang, C.; Bethune, D.; Heben, M. *Nature* **1997**, *386*, 377.
(31) Ye, Y.; Ahn, C.; Witham, C.; Fultz, B.; Liu, J.; Rinzler, A.; Colbert, D.; Smith, K.; Smalley, R. *Appl. Phys. Lett.* **1999**, *74*, 2307.
(32) Talapatra, S.; Zambano, A.; Weber, S.; Migone, A. *Phys. Rev. Lett.* **2000**, *85*, 138.
(33) Muris, M.; Dufau, N.; Bienfait, M.; Dupont-Pavlovsky, N.; Grillet, Y.; Palmari, J. *Langmuir* **2000**, *16*, 7019.
(34) Bienfait, M.; Asmussen, B.; Johnson, M.; Zeppenfeld, P. *Surf. Sci.* **2000**, *460*, 243.
(35) Keffer, D.; McCormick, A. V.; Davis, H. T. *J. Phys. Chem.* **1996**, *100*, 967.
(36) Keffer, D.; Davis, H. T.; McCormick, A. V. *Adsorption* **1996**, *2*, 9.
(37) Levitt, D. G. *Phys. Rev.* **1973,** *A8*, 3050.
(38) Bennett, J. M.; Cohen, J. P.; Flanigen, E. M.; Pluth, J. J.; Smith, J. V. *ACS Symp. Series* **1983**, *218*, 109.
(39) Hahn, K.; Karger, J.; Kukla, V. *Phys. Rev. Lett.* **1996**, *76*, 2762.
(40) Gergidis, L.; Theodorou, D.; Jobic, H. *J. Phys. Chem. B* **2000**, *104*, 5541.
(41) Jirage, K.; Hulteen, J.; Martin, C. *Science* **1997**, *278*, 655.
(42) Sinnott, S. B.; Qi, L.; Shenderova, O. A.; Brenner, D. W. *Molecular Dynamics of Clusters, Surfaces, Liquids, and Interfaces*; Hase, W., Ed.; JAI Press: Stamford, Connecticut, 1999; Chapter 1.
(43) Brenner, D. W. *Phys. Stat. Solidi B* **2000**, *217*, 23.
(44) Ryckaert, J.; Bellemans, A. *Chem. Phys. Lett.* **1975**, *30*, 123.
(45) Sinnott, S. B.; Shenderova, O. A.; White, C. T.; Brenner, D. W. *Carbon* **1998**, *36*, 1.
(46) Saito, R.; Dresselhaus, G. *Physical Properties of Carbon Nanotubes*, Imperial College Press: London, 1998.
(47) Mao, Z.; Garg, A.; Sinnott, S. B. *Nanotechnology* **1999**, *10*, 273.
(48) Bird, R.; Stewart, W.; Lightfoot, E. *Transport Phenomena*, John Wiley & Sons: New York, 1976.
(49) Haile, J. *Molecular Dynamics Simulations: Elementary Methods*, Wiley-Interscience: New York, 1992.
(50) Benes, N.; Verweij, H. *Langmuir* **1999**, *15*, 8292.
(51) Sanborn, M.; Snurr, R. *Sep. and Purif. Technol.* **2000**, *20*, 1.
(52) MacElroy, J.; Boyle, M. *Chem. Eng. J.* **1999**, *74*, 85.
(53) Bouyermaouen, A.; Bellemans, A. *J. Chem. Phys.* **1998**, *5*, 2170.
(54) Skoulidas, A.; Sholl, D. *J. Phys. Chem. B*, in press.
(55) Sholl, D.; Lee, C. *J. Chem. Phys.* **2000**, *112*, 817.